Phonon free energy and devil's staircases in the origin of polytypes

M J Rutter and Volker Heine

Cavendish Laboratory (TCM), Madingley Road, Cambridge CB3 0HE, UK

Abstract.   Phase transitions in polytypic substances can display a rich structure. A polytypic material, being formed from stacked layers, each layer having freedom of orientation, has an infinite number of possible structures. Thus a phase transition between two simple structures could occur directly, or via an infinite sequence of intermediate phases. Such a sequence, called a 'devil's staircase', can arise from simple and general mathematical models. This paper presents a simple model in which the phonon free energy drives a temperature-induced phase transition, the mechanism which is believed to cause phase transitions in SiC, CdI_2 and PbI_2. The form of interaction between changes in the stacking orientation caused by the phonon free energy is found to be inversely proportional to the square of the separation of the changes, but of alternating sign. Although no staircase results from this interaction, one intermediate phase does arise, and others are barely unstable.

1. Introduction

Over many decades there has been much interest in polytypic materials and reasons for the occurrence of the polytypes. Good reviews of the state of knowledge in 1966 and 1983 respectively are given by Verma and Krishna [1] and Krishna [2]. In some systems there is a reasonably widely accepted mechanism for polytype formation, such as via giant screw dislocations in zinc sulphide [3, 4], but similar work on silicon carbide is less conclusive [5, 6]. Jagodzinski [7] suggested that the phonon free energy could be important in polytype stabilization, and this effect has subsequently been shown to be important in SiC [8, 9] and PbI_2 [10]. However, in general there is still much uncertainty as to which polytypes are stable phases, which merely growth phenomena, and what mechanisms stabilize them. The phase diagram is often unclear due to long annealing times, and the influence that dislocations and impurities may have over the phase grown.

The purpose of the present work is to consider further the role of the phonon free energy in the stabilization of polytypes. In particular we consider its role in the higher-order polytypes with complex stacking sequences and long unit cells. The investigation has been stimulated by noting some similarities to and differences from the mathematical model of Bak and Bruinsma [11], which gives an infinite sequence ('devil's staircase') of complex stable phases, as discussed below.

Polytypes usually arise when a crystal structure is formed of layers, each of which can take one of two (or more) orientations without dramatically affecting the bonding structure. Examples include CdI_2, PbI_2 and SiC.

For simplicity we shall consider a model similar to SiC, where each layer can be stacked in one of two orientations, related by a $180°$ rotation (figure 1), but we believe the results
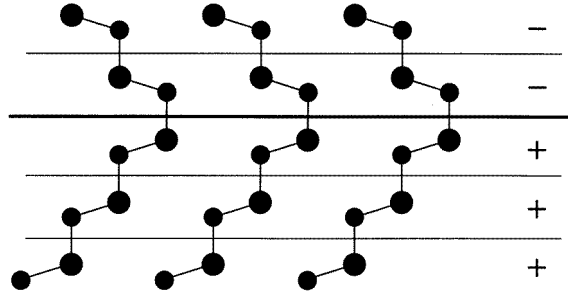
Figure 1. A diagram of a simple polytype showing layers in two orientations denoted $+$ and $-$. If this were the repeat unit, the polytype would be called $\langle 23 \rangle$. The stacking boundary is highlighted.

to be more general. It is convenient to refer to the two orientations as '$+$' or '$-$' layers (figure 1), and a change in orientation as a 'stacking boundary.' We shall adopt the Zhdanov notation [12] for the resulting polytypes, which simply counts the number of layers between stacking boundaries in the repeat unit. Thus the sequence '$+--+--$' would be called $\langle 12 \rangle$, and '$+-+-+-$' $\langle 11 \rangle$ or simply $\langle 1 \rangle$. The cubic structure, in which all layers have the same orientation, is denoted $\langle \infty \rangle$

In previous work on polytypes [8, 13], the energy or free energy of a system has been described by a sum over the layers as

$$E = J_0 N - \sum_{i,n} J_n \sigma_i \sigma_{i+n} - \sum_{i,n,m,o} K_{n,m,o} \sigma_i \sigma_{i+n} \sigma_{i+m} \sigma_{i+o} + \cdots \tag{1}$$

where $\sigma_i = \pm 1$ depending on the orientation of the ith layer and N is the number of layers. Here J_0 is the self-energy of a layer, J_n the pairwise interaction, and $K_{n,m,o}$ a four-layer interaction. There are no terms for the interaction of an odd number of layers, as the energy must be unchanged on reversing the sign of all of the σ_i—that is, simply rotating the crystal. This form has been discussed critically by Shaw and Heine [14], and is an extension of the more restrictive ANNNI model, which has $J_n = 0$ for $n > 2$. A review of polytypism in general under the ANNNI model is given by Yeomans [15]. The full ANNNI model includes nearest-neighbour interactions within the planes perpendicular to the stacking axis, whereas as can be seen from figure 1, all atoms within a layer must take the same orientation in the structure considered here—the energy cost of a kink on the stacking boundary would be prohibitively large.
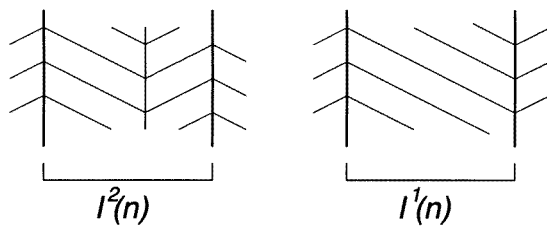
Figure 2. Contrasting nearest-neighbour and next-nearest-neighbour interactions, and showing the two different orientations of boundary. Note the change of orientation of the figure with respect to figure 1.

The energy can also be expressed through consideration of the presence or absence of a boundary, rather than the orientation of a layer. Just as there are two orientations for a layer, there are also two orientations for a boundary, figure 2, and we note that the interaction between like and unlike boundaries may be different. At every position at which a boundary could occur a variable η can be defined, taking the value zero if there is no boundary, or ± 1 according to the type of boundary. The energy can then be expressed as

$$E = J_0 N + I_0 N_b - \sum_{i,n} I_n \eta_i \eta_{i+n} + \cdots \tag{2}$$

where N_b is the number of boundaries, I_0 is the self-energy of a boundary, and I_n describes the pairwise boundary interaction.

If equation (1) contains only pairwise terms, and no higher terms, then this description in terms of boundaries also needs no terms higher that the pairwise term [8], and the boundary interaction I_n can be related to the layer interaction J_n. In this case, with $I^j(n)$ defined to be the interaction between two boundaries of separation n and with $j - 1$ intervening boundaries, then

$$I^j(n) = (-1)^{j+1} I^1(n). \tag{3}$$

This follows directly from equation (2) because neighbouring boundaries must be of opposite type (figure 2), and thus the product $\eta_i \eta_j$ will be -1 if i and j refer to neighbouring boundaries, or boundaries with an even number of intervening boundaries, and $+1$ if the number of intervening boundaries is odd. This simple alternation in the sign of the interaction can be emphasized by denoting $I^1(n)$ as simply $I(n)$, and then equation (2) can be written in terms of a sum over boundary pairs as

$$E = J_0 N + I_0 N_b + \sum_{\text{pairs}} (-1)^{j+1} I(n). \tag{4}$$
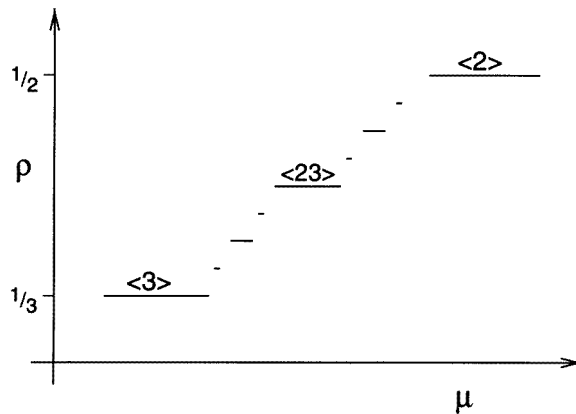
Figure 3. The density ρ of boundaries per unit length in a phase transition from $\langle 2 \rangle$ to $\langle 3 \rangle$ via an infinite staircase of intermediate phases as a function of some parameter μ.

Consider a phase transition between two simple structures such as from $\langle 2 \rangle$ to $\langle 3 \rangle$ as a function of temperature or other external variable such as pressure. It need not be a single sharp transition but it could occur via intermediate phases, each stable over its own range of temperatures. Indeed, the number of intermediate phases could be infinite, producing what is called a 'devil's staircase'. This is shown schematically in figure 3, where an

infinite number of phases, characterized by ρ, occurs across a transition region between two end-point phases as an external parameter μ is varied. Such a staircase can arise from remarkably simple mathematical models [11, 16]. For instance, if identical entities are placed on a grid, and they interact via a potential which is convex, repulsive, pairwise and infinite-ranged, a staircase will result, as was shown by Bak and Bruinsma [11].

In polytypic phase transitions, the stacking boundaries can be considered to be the entities of the Bak–Bruinsma model, and in this paper the interaction is considered to occur via differences in the phonon free energy. However, the entities are not identical, as there are two types of stacking boundary, and hence do not map directly onto the Bak–Bruinsma model.

In this paper we consider simple structures in one, two and three dimensions, and a simple representation of the interatomic forces by springs between nearest-neighbour point masses. The model structures support stacking boundaries similar to those in figure 1, and their phonon spectra and free energies can be readily calculated and analysed. The calculations are much simpler than using a full shell model for the atomic interactions, so the results can be obtained for systems with longer repeat distances, and hence long-range boundary interactions studied. Computations on systems with a repeat distance of over one hundred atoms can be carried out in less than an hour on a modest work-station with the models presented here.

These models are used to find the boundary self-energy and interaction energy as a function of separation. Once this has been done, the energy of much larger systems can be calculated by using equation (4) directly. Energies of systems of 10^5 layers can be calculated in a few seconds of computer time from this equation, and thus in a two-step process the study of truly long-period polytypes is facilitated.

The simplest model would be that of a one-dimensional (1D) chain of balls and springs. This supports phonons and has a corresponding phonon free energy, and boundaries can be simulated by introducing the scattering perturbation of a changed mass or spring constant. However, as is shown in the appendix, the resulting change in the phonon free energy is independent of the relative position of the changed masses or spring constants, and hence they do not interact. The 1D case will therefore not be considered further.
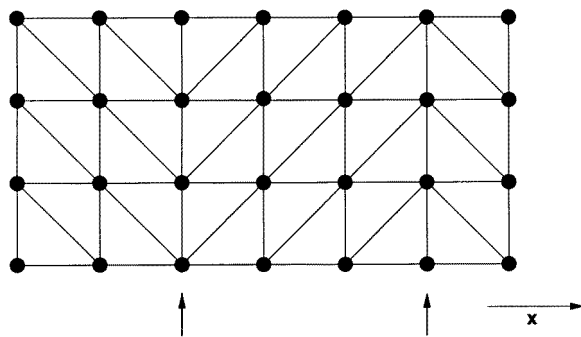
Figure 4. A simple 2D ball-and-spring model showing stacking reversals. The lines represent springs. Note the two boundaries indicated by the arrows.

The next-simplest model considered is a two-dimensional ball-and-spring system. In two dimensions it is possible to place springs in different orientations in different columns, and thus produce a structure more closely analogous to a polytypic structure. As shown

in figure 4, a square mesh is used in which each column has one diagonal link per cell, sufficient to prevent zero-frequency modes, and sufficient to define an orientation for each column. The figure shows two changes in orientation, or stacking boundaries. Comparison with figure 1 shows that the structure is analogous to that of SiC.

We believe that our results have a much wider generality than the simplified model that we have used. With identical masses and spring constants everywhere, and no bond-bending term in its energy, this model is quite a long way removed from a real polytypic crystal, although the essential symmetry properties have been retained. However, the system could be analysed in terms of lattice waves travelling in perfect crystalline material, reflected and diffracted at the stacking boundaries. The nature of the phonon spectra and the matching conditions at boundaries are qualitatively universal, and thus we expect our results to be.

Extension to three dimensions is really necessary in order to move closer to the phonon spectra of real crystals, and this is included in subsequent sections of this paper.

2. Methodology and interaction

2.1. Methodology

The approach taken in determining the form of the boundary–boundary interaction can be considered in the following steps. The free energy of a boundary-free system is found, and then the variation in energy for a system of two boundaries as their separation is varied. Thus the boundary self-energy and nearest-neighbour interaction can be deduced. Then the next-nearest-neighbour interaction is calculated by considering a group of three boundaries, and this result is compared with a theoretical prediction based on the nearest-neighbour result. Finally, the energies of some short-period polytypes are calculated, the model derived from the first steps above re-fitted to these data, and the consistency checked.

All of these steps use the high-temperature limit of the phonon free energy, which is as follows:

$$F_\phi = kT \sum_n \ln\left(2\sinh\left(\frac{\hbar\omega_n}{2kT}\right)\right) \approx N_\phi kT \ln\left(\frac{\hbar}{kT}\right) + \frac{1}{2}kT\,\Xi \tag{5}$$

where

$$\Xi = \sum_n \ln(\omega_n^2) \tag{6}$$

and N_ϕ is the number of non-zero-frequency phonon modes, $(N-1)d$ in d dimensions.

The only term in this equation which depends on the polytype is Ξ. Thus when comparing the free energies of different polytypes, the other terms can be ignored.

Because the important free-energy differences are related to differences in the logarithms of the eigenfrequencies, a uniform scaling of all of the eigenfrequencies produces no change at all in the free-energy differences. Hence the choice of mass or spring constant is irrelevant, and unity was used for both.
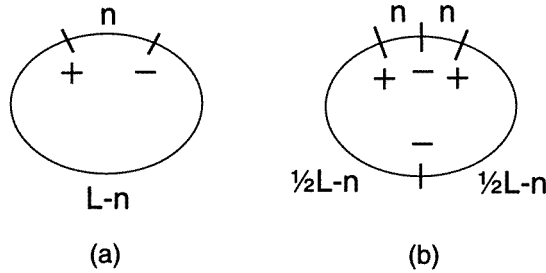
2.2. 2D interaction

Firstly Ξ was calculated for a 120×48 grid with periodic boundary conditions and no stacking boundaries. All of the calculations were done on a 120×48 grid, and this value represents the energy of a boundary-free system, and will be denoted Ξ_0. All other values for Ξs quoted have this grid self-energy of just under 8700 subtracted.

By calculating the energies of various systems with stacking boundaries, it is hoped that a formula such as

$$\Xi = \Xi_0 + N_b A_b I_0 + A_b \sum_{i,j} I^{j-i}(r_i - r_j) \tag{7}$$

can be applied, where N_b is the number of boundaries, A_b their area, and I_0 and $I^j(n)$ the self-energy and interaction energy of boundaries as described in section 1. The stacking direction is chosen to be along the longer, 120-unit direction, so A_b is 48. A_b is extracted from I_0 and $I(n)$ to leave a quantity which should be almost independent of system size. Once the form of $I^j(n)$ has been found, the full two- or three-dimensional phonon calculation can be reduced to a simple interaction on a one-dimensional system.

Figure 5. Systems with (a) a pair and (b) a triplet of boundaries used in determining nearest-neighbour and next-nearest-neighbour interactions. A fourth boundary is required with the triplet, as the boundaries must alternate in type. Here L is the length of the system in the x-direction, the closed loop indicating the use of periodic boundary conditions.

On such a periodic system, the number of boundaries must be even, as shown by figure 5, so the simplest systems that can be considered are those with two and four boundaries.

Considering a system with just a pair of boundaries of separation n on a grid of length L and periodic boundary conditions, the value of Ξ will be given by

$$\Xi(\text{pair}; n) = A_b(2I_0 + I^1(n) + I^1(L - n) + 2I^2(L) + I^3(L + n) + \ldots) \tag{8}$$

where $\Xi(\text{pair}; n)$ is the value of $\Xi - \Xi_0$ for a system with a pair of boundaries separated by n. This can be approximated as

$$\Xi(\text{pair}; n) \approx A_b(2I_0 + I^1(n)). \tag{9}$$

Figure 6 shows a fit of this equation to computed data points for n between 1 and 10 assuming that

$$I(n) = a/n \tag{10}$$

where a and I_0 are the only fitting parameters. The fit is extremely good, as can be seen, and this is the only justification offered here for the functional form chosen. The values produced from the fit are $I_0 = 0.121\,968$ and $a = -0.046\,493$. The nearest-neighbour interaction is seen to be attractive, in contrast to that required for a Bak–Bruinsma staircase.

Having thus found the nearest-neighbour interaction, we now seek the next-nearest-neighbour interaction. This is obtained through consideration of a triplet of boundaries, as shown in figure 5. Again considering just the most important terms contributing to Ξ, and removing Ξ_0,

$$\Xi(\text{triplet}; n) \approx A_b(4I_0 + 2I^1(n) + I^2(2n)) \tag{11}$$
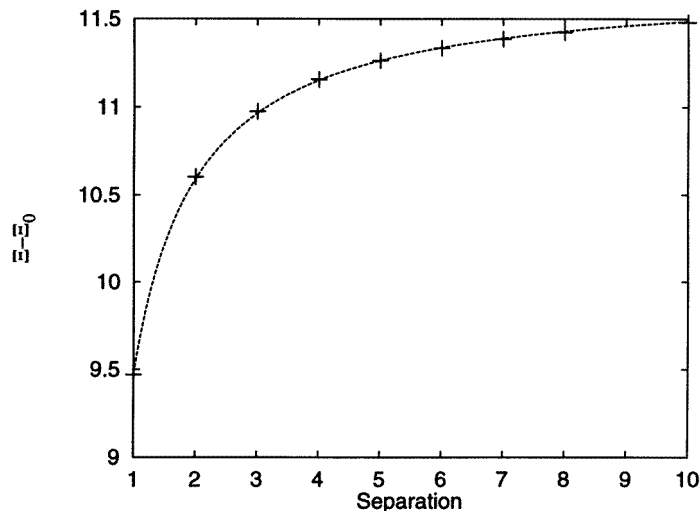
Figure 6. $\Xi - \Xi_0$ in 2D as a function of the boundary separation n for an isolated pair of boundaries on a 120×48 grid, and a fit of $A_b(2I_0 + a/n)$.

or

$$I^2(2n) \approx (\Xi(\text{triplet}; n) - 2\Xi(\text{pair}; n))/A_b. \tag{12}$$

As we expect from equation (3) that

$$I^2(n) \approx -I^1(n) \tag{13}$$

table 1 is constructed to test this theory.

Table 1. Calculation of next-nearest-neighbour interactions in 2D, and comparison with nearest-neighbour interactions.

n	$\Xi(\text{pair}; n)$	$\Xi(\text{triplet}; n)$	$A_b I^2(2n)$	$-A_b I^1(2n)$	Difference
1	9.469 743	20.137 265	1.197 778	1.104 695	7.77%
2	10.604 305	21.842 675	0.634 064	0.554 107	12.61%
3	10.974 105	22.394 945	0.446 736	0.374 629	16.14%
4	11.154 893	22.660 211	0.350 425	0.284 108	18.92%
5	11.262 581	22.814 170	0.289 007	0.228 215	21.03%

This table agrees broadly with the prediction, being correct in sign and to within 25% in magnitude. For the purposes of correcting the error from the omitted terms, it would now be justifiable to assume that equation (13) is correct, and that the intervening boundary has just caused a change of the sign of $I^j(n)$. The next-nearest-neighbour interaction is therefore repulsive.

Returning to the pair of boundaries, equation (8) can now be approximated as

$$\Xi(\text{pair}; n) \approx A_b \left(2I_0 + I^1(n) + n^2 \left. \frac{\partial^2 I(x)}{\partial x^2} \right|_L + \cdots \right). \tag{14}$$

Thus equation (9) was a better approximation to equation (8) than could have been initially justified, because the omitted terms tend to cancel.

For the triplet structure the cancellation is not complete. Indeed, the group of three boundaries acts like a single boundary when viewed from a long distance, so we have

$$\Xi(\text{triplet}; n) = A_b(4I_0 + 2I^1(n) + I^2(2n) + 2I(L/2)). \tag{15}$$

A new table for $I^2(n)$ can then be produced from the formula

$$I^2(2n) \approx (\Xi(\text{triplet}; n) - 2\Xi(\text{pair}; n) - \Xi(\text{pair}; L/2))/A_b + 2I_0. \tag{16}$$

With this correction in place, table 2 is produced. The agreement now is very good between the calculated free energy of the triplet system, and that predicted from the pairwise interactions. This adds considerable justification to equation (3).

Table 2. More refined calculation of next-nearest-neighbour interactions in 2D, and comparison with nearest-neighbour interactions.

n	$\Xi(\text{pair}; n)$	$\Xi(\text{triplet}; n)$	$A_b I^2(2n)$	$-A_b I^1(2n)$	Difference
1	9.469 743	20.137 265	1.131 678	1.104 695	2.38%
2	10.604 305	21.842 675	0.567 964	0.554 107	2.44%
3	10.974 105	22.394 945	0.380 636	0.374 629	1.58%
4	11.154 893	22.660 211	0.284 325	0.284 108	0.08%
5	11.262 581	22.814 170	0.222 907	0.228 215	−2.38%

Calculation of further interactions, such as $I^3(n)$, becomes increasingly difficult as systems which contain the term of interest also contain an increasing number of other, larger terms. Equation (3) suggests that the interaction should continue to alternate in sign, and as a simple test of this $I^3(n)$ is calculated from the value of Ξ for a group of four boundaries, each a distance n from its neighbours:

$$\Xi(\text{quad}; n) \approx 4I_0 + 3I^1(n) + 2I^2(2n) + I^3(3n) \tag{17}$$

all terms of the form $I(L)$ tending to cancel. Just $I^3(3)$ and $I^3(6)$ were calculated in this way, and the result agreed with equation (3) in sign and to within $12\frac{1}{2}\%$ in magnitude.

Rather than continuing to consider groups of five, six, seven and more boundaries, this analysis of interactions beyond $I^2(n)$ is concluded by considering Ξ for a grid full of boundaries at constant separation, which can be calculated and fitted independently of the above results. With a grid length, L, of 120, it is possible to place boundaries at separations of 2, 3, 4, 5, 6, 10, 12, 15, 20, 30, and 60 units, and equation (7) takes the form

$$\Xi - \Xi_0 = LA_b I_0/n + \frac{LA_b}{n} \sum_j I^{j-1}(r_1 - r_j) \tag{18}$$

as all of the boundaries are identical. Fitting yields an I_0 of 0.1218 and an a of $-0.044\,83$— both within 4% of the previously calculated values. A table of these data is given as table 3. This is an independent fitting producing an independent check on the previous values for I_0 and a.

These results for 2D can be summarized by saying that equation (7) applies with

$$I^j(n) = (-1)^{j+1} \frac{a}{n}. \tag{19}$$

$I_0 = 0.122$ and $a = -0.046\,49$, using the results from the isolated pairs, as these results are less sensitive to the approximation that $I^2(n) = -I^1(n)$.

Table 3. An independent fit of equation (18) to a grid full of uniformly spaced boundaries.

Boundary spacing	$\Xi - \Xi_0$	Fitted result
2	305.971	306.059
3	214.154	213.982
4	164.302	164.215
5	133.182	133.161
6	111.940	111.962
10	68.266	68.3702
12	57.100	57.2237
15	45.842	45.9778
20	34.513	34.6325
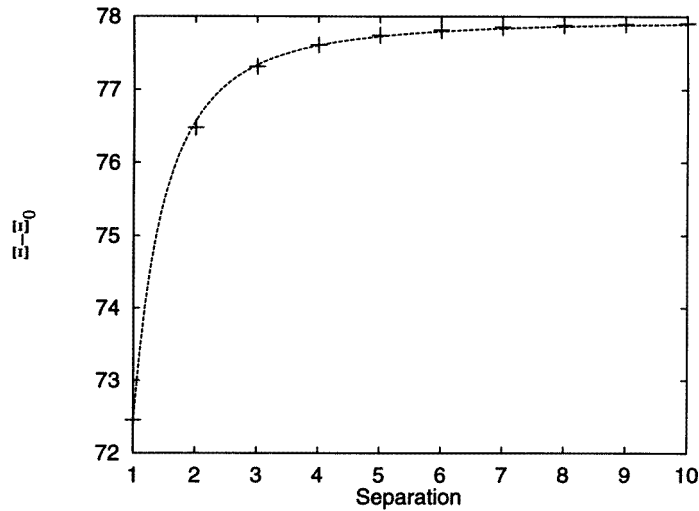
Figure 7. $\Xi - \Xi_0$ in 3D as a function of the boundary separation n for an isolated pair of boundaries on a $120 \times 29 \times 29$ grid, and a fit of $A_b(2I_0 + a/n^2)$.

2.3. 3D interaction

The above analysis can be repeated for the analogous 3D structure. We take layers of figure 4, retaining x as the unique axis, and stack them on top of one another in the z-direction perpendicular to the page. In order to stabilize the structure, two diagonal springs are added across every square in the yz- and xz-planes.

The calculation of the nearest-neighbour interaction follows from the free energy of a system of the type shown in figure 5(a). A grid size of $120 \times 29 \times 29$ is now used, and the results are shown in figure 7, fitted extremely well by the function

$$\Xi - \Xi_0 = A_b \left(2I_0 + \frac{a}{n^2} \right) \tag{20}$$

with $I_0 = 0.046\,343$ and $a = -0.006\,561$.

The interaction with a second-neighbour boundary is determined again from equation (16), and is compared with $-I^1(n)$ in table 4. The agreement is not as good as in the 2D system, indicating that the approximation of equation (13) does not apply as closely in 3D as in 2D.

Table 4. Calculation of next-nearest-neighbour interactions in 3D, and comparison with nearest-neighbour interactions.

n	Ξ (pair; n)	Ξ (triplet; n)	$A_b I^2 (2n)$	$-A_b I^1 (2n)$	Difference
1	72.455 285	146.581 542	1.555 471	1.471 855	5.38%
2	76.478 145	153.437 573	0.365 784	0.338 992	7.32%
3	77.314 939	154.890 294	0.144 917	0.136 557	5.77%
4	77.611 008	155.409 684	0.072 169	0.072 406	−0.33%
5	77.744 361	155.642 762	0.038 540	0.043 356	−12.50%

Once more the energy of a grid full of a polytype can be calculated, and the result fitted by an equation of the form of equation (18). This gives values corresponding to $I_0 = 0.046\,362$ and $a = 0.007\,063$. This provides reasonable independent agreement with the previous values of $I_0 = 0.046\,343$ and $a = -0.006\,561$. Exact agreement is not expected because of the assumption inherent in equation (3) that the interaction simply alternates in sign as intervening boundaries are traversed, which is an approximate result.

3. Phase diagrams

After the above work in finding the form of Ξ, the total free energy of the system can now be expressed as

$$F_{tot} = F_0 + \frac{1}{2} kT \Xi + N E_{el} \tag{21}$$

where N is the number of atoms, and E_{el} represents an electronic, that is a non-phonon contribution to F_{tot}. In SiC such a term has been the subject of calculations by Cheng *et al* [17] and Käckell *et al* [18]. Such a term can prevent the boundaries from coalescing and disappearing, for it can provide strong short-range repulsion.

Choosing to focus on the $\langle 2 \rangle$-to-$\langle 3 \rangle$ transition which is so important in SiC, and assuming that electronic interactions do not extend beyond four layers, E_{el} can be written as

$$E_{el} = 3 E_{el, \langle 3 \rangle} - 2 E_{el, \langle 2 \rangle} + 6 \rho [E_{el, \langle 2 \rangle} - E_{el, \langle 3 \rangle}] \tag{22}$$

where ρ is the linear density of boundaries. In this case the electronic energies $E_{el, \langle 2 \rangle}$ and $E_{el, \langle 3 \rangle}$ are almost identical, whereas $E_{el, \langle 1 \rangle}$ and $E_{el, \langle 4 \rangle}$ are significantly higher, and thus prevent the boundaries from occurring at separations other than two or three. Defining $\tilde{F}$ as a shifted F per atom, with the terms independent of polytypes removed from both the phonon and electronic free energies, we have

$$\tilde{F} = \frac{1}{2} kT \left(\rho I_0 + \frac{1}{N} \sum_{i,j} I^{j-i} (r_i - r_j) \right) - \rho \, \Delta E_{el} \tag{23}$$

where r_i is the position of the ith boundary, and

$$\Delta E_{el} = 6 [E_{el, \langle 3 \rangle} - E_{el, \langle 2 \rangle}]. \tag{24}$$

It is then possible to consider $\tilde{F}$ for each polytype in the limit of infinite system size by defining the polytype-dependent sum

$$S_{\langle \, \rangle} = \lim_{N \to \infty} \frac{1}{N} \sum_{i,j} I^{j-i} (r_i - r_j) \tag{25}$$

so that

$$\tilde{F}_{(\ )} = \frac{1}{2}kT(\rho I_0 + S_{(\ )}) - \rho \Delta E_{el}. \tag{26}$$

The stable polytype at a given T will be the one with the minimum $\tilde{F}$ and hence the minimum F.

The electronic term ΔE_{el} is necessary to produce any phase transitions at all. Without it, all polytypes have the same free energy at $T = 0$, and nowhere else.

From the results for the form of $I^j(n)$, it is now possible to calculate $\rho I_0 + S_{(\ )}$ for various polytypes in two and three dimensions. This is shown in table 5 for the two-dimensional case.

Table 5. Phonon contribution to the free energy of various polytypes in 2D.

Polytype	ρ	$\rho I_0 + S_{()}$
$\langle 2 \rangle$	$\frac{1}{2}$	0.052 927
$\langle 2223 \rangle$	$\frac{4}{9}$	0.047 597
$\langle 23 \rangle$	$\frac{2}{5}$	0.043 306
$\langle 233 \rangle$	$\frac{3}{8}$	0.040 990
$\langle 232333 \rangle$	$\frac{3}{8}$	0.040 978
$\langle 2333 \rangle$	$\frac{4}{11}$	0.039 918
$\langle 3 \rangle$	$\frac{1}{3}$	0.037 075

Two of the polytypes selected in this table have the same value of ρ. For this pair, the one with the lower $S_{(\ )}$ or $\rho I_0 + S_{(\ )}$ will be stable with respect to the other at all temperatures, as the electronic contribution depends on ρ only. Thus $\langle 232333 \rangle$ is stable with respect to $\langle 233 \rangle$. This follows the suggestion of Cheng *et al* [8] that this sort of interaction will favour polytypes with an even number of layers in their repeat structure—that is, an even number of symbols in their Zhdanov notation.

Two phases a and b will be in equilibrium if they have the same $\tilde{F}$, that is if

$$\frac{1}{2}kT(\rho_{\langle a \rangle} I_0 + S_{\langle a \rangle}) - \rho_{\langle a \rangle} \Delta E_{el} = \frac{1}{2}kT(\rho_{\langle b \rangle} I_0 + S_{\langle b \rangle}) - \rho_{\langle b \rangle} \Delta E_{el} \tag{27}$$

or

$$T = \frac{2 \Delta E_{el}(\rho_{\langle a \rangle} - \rho_{\langle b \rangle})}{k(\rho_{\langle a \rangle} I_0 + S_{\langle a \rangle} - \rho_{\langle b \rangle} I_0 - S_{\langle b \rangle})}. \tag{28}$$

Hence ΔE_{el} sets the scale for T. If $\Delta E_{el} = 0$ there is no phase diagram, and for positive transition temperatures ΔE_{el} must be positive, because the sign of the denominator is dominated by the I_0-terms where I_0 is positive. For convenience when plotting the phase diagram, two reduced variables are introduced:
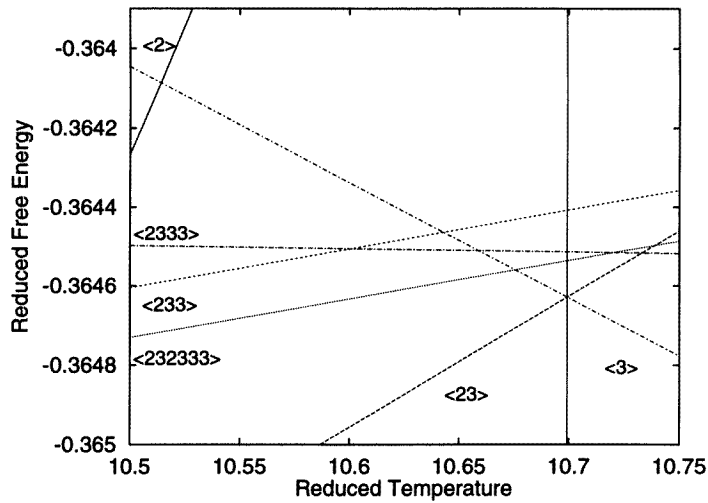
$$T' = \frac{kT}{2 \Delta E_{el}}$$
$$\tilde{F}' = \frac{\tilde{F}}{\Delta E_{el}} \tag{29}$$

so that

$$\tilde{F}'_{(\ )} = T'(\rho I_0 + S_{(\ )}) - \rho. \tag{30}$$
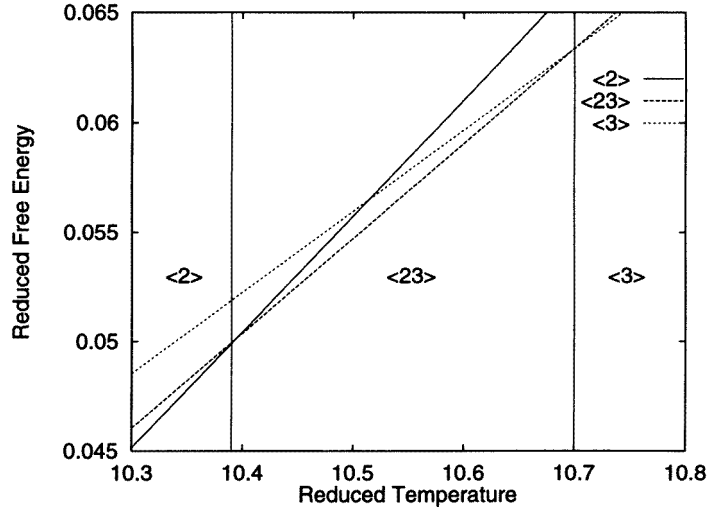
Figure 8. The phase diagram from the 2D interaction showing $\langle 2 \rangle$, $\langle 23 \rangle$ and $\langle 3 \rangle$ and their regions of stability, in terms of the reduced variables defined in equation (29).

Figure 9. Detail of the transition from $\langle 23 \rangle$ to $\langle 3 \rangle$ for the 2D case. There is no intermediate phase here. A linear term, $0.04T'$, has been removed from all lines.

The reduced free energies of several polytypes in 2D are shown in figures 8 and 9. The figures show that $\langle 23 \rangle$ does have a short range of stability, whereas the other intermediate phases do not. In this case the fractional width of the region of stability of $\langle 23 \rangle$—that is, ΔT divided by the transition temperature—is about 0.03. If therefore ΔE_{el} were such that the transition occurred at around 2400 K, $\langle 23 \rangle$ would be stable over about 70 K.

For the $\pm n^{-2}$-interaction for 3D, the results are qualitatively the same, in that $\langle 23 \rangle$ is still stable, and only $\langle 23 \rangle$ is stable between $\langle 2 \rangle$ and $\langle 3 \rangle$, but the stability range is significantly smaller, with $\Delta T/T_0$ only 0.006. The free-energy difference in this case between $\langle 23 \rangle$ and

a mixture of $\langle 2 \rangle$ and $\langle 3 \rangle$ is very small—around $5 \times 10^{-6} kT$. This is still significant, for the stacking boundaries are forced to be flat due to the very high energy penalty, of the order of eV, of creating any kink on them. Thus all of the atoms within one layer—a figure which could easily be over one million—act as a single unit in respect of this degree of freedom. The energy change on reorienting this unit is therefore greater than kT.

4. The phase $\langle n \, n + 1 \rangle$

Having shown for two specific cases that $\langle 23 \rangle$ occurs as an intermediate phase between $\langle 2 \rangle$ and $\langle 3 \rangle$, it is natural to wonder whether this result is more general. Indeed it is, and there follows a proof that the phase $\langle n \, n + 1 \rangle$ will occur between the phases $\langle n \rangle$ and $\langle n + 1 \rangle$ for interactions of the form

$$I^j(n) = (-1)^{j+1} n^{-\alpha} \tag{31}$$

for integer values of α between one and four, and probably all positive α. The proof for $\alpha = 1$ follows.

The free energy of a polytype $\langle n \rangle$ is given by

$$\tilde{F}_{\langle n \rangle} = \frac{1}{2} kT (\rho_{\langle n \rangle} I_0 + S_{\langle n \rangle}) - \rho_{\langle n \rangle} \Delta E \tag{32}$$

and there must exist some T_c at which $\tilde{F}_{\langle n \rangle} = \tilde{F}_{\langle n+1 \rangle}$—that is, at which $\langle n \rangle$ and $\langle n + 1 \rangle$ are mutually in equilibrium.

At this T_c, a system can exist which is partially $\langle n \rangle$ and partially $\langle n+1 \rangle$. Such a system, consisting of a fraction χ of $\langle n \rangle$ and $1 - \chi$ of $\langle n + 1 \rangle$ would have a free energy given by

$$\tilde{F}_{\text{mix}} = \frac{1}{2} kT_c (\rho I_0 + \chi S_{\langle n \rangle} + (1 - \chi) S_{\langle n+1 \rangle}) - \rho \, \Delta E \tag{33}$$

where ρ is simply the density of the boundaries in the mixture. If $\chi = n/(2n + 1)$ then ρ is the same as that for the polytype $\langle n \, n + 1 \rangle$. If $\langle n \, n + 1 \rangle$ is to be stable, its free energy must be less than that of the mixture of $\langle n \rangle$ and $\langle n + 1 \rangle$. In other words

$$S_{\langle n \, n+1 \rangle} < \frac{n}{2n + 1} S_{\langle n \rangle} + \frac{n + 1}{2n + 1} S_{\langle n+1 \rangle}. \tag{34}$$

Considering the case of the $\pm 1/n$ interaction—that is, the 2D case—and ignoring the multiplicative constant a in the definition of $S_{(\ )}$ (equation (25)), we have

$$
\begin{aligned}
S_{\langle n \rangle} &= -\frac{1}{n} + \frac{1}{2n} - \frac{1}{3n} + \frac{1}{4n} - \cdots \\
S_{\langle n+1 \rangle} &= -\frac{1}{n + 1} + \frac{1}{2n + 2} - \frac{1}{3n + 3} + \frac{1}{4n + 4} - \cdots \\
2S_{\langle n \, n+1 \rangle} &= -\frac{1}{n} + \frac{1}{2n + 1} - \frac{1}{3n + 1} + \frac{1}{4n + 2} \\
&\quad - \frac{1}{n + 1} + \frac{1}{2n + 1} - \frac{1}{3n + 2} + \frac{1}{4n + 2} - \cdots.
\end{aligned}
\tag{35}
$$

These expressions may be manipulated to give

$$\frac{2n}{2n + 1} S_{\langle n \rangle} + \frac{2n + 2}{2n + 1} S_{\langle n+1 \rangle} = -\frac{2}{n + \frac{1}{2}} + \frac{2}{2n + 1} - \frac{2}{3n + \frac{3}{2}} + \frac{2}{4n + 2} - \cdots \tag{36}$$

and

$$2S_{\langle n \, n+1 \rangle} = -\frac{1}{n} - \frac{1}{n + 1} + \frac{2}{2n + 1} - \frac{1}{3n + 1} - \frac{1}{3n + 2} + \frac{2}{4n + 2} - \cdots. \tag{37}$$

Performing the comparison termwise, the condition for $\langle n\, n+1 \rangle$ being stable reduces to

$$-\frac{1}{n} - \frac{1}{n+1} < -\frac{2}{n+\frac{1}{2}} \tag{38}$$

and similar forms, all of which are clearly true. Thus $\langle n\, n+1 \rangle$ is a stable with respect to $\langle n \rangle$ and $\langle n+1 \rangle$ at some temperature for the $\pm 1/n$ interaction.

This analysis can be repeated for other interactions, and one of the authors (MJR) has repeated it for $\pm n^{-\alpha}$ for α equal to 2, 3 and 4 with the aid of computer-assisted algebra. The conclusion is that $\langle n\, n+1 \rangle$ always has a stability range. The important value of α is 2, that corresponding to 3D.

5. Conclusions

Previous work has shown that phonon free energy can cause phase transitions between polytypes. In this work the interaction between adjacent stacking boundaries, $I^1(n)$ has been obtained to much greater distances than before through the use of a simplified model, and has been shown to depend on n as $-a/n$ in 2D and $-a/n^2$ in 3D for moderate values of n (1 to 10). We have also shown that $I^2(n) = -I^1(n)$ as previously predicted [8].

Although further interactions, such as $I^3(n)$, are progressively more difficult to calculate, data do suggest that $I^3(n) \approx I^1(n)$ in the 2D case. In 3D the calculation is more prone to errors, as the most significant I^3-term occurs when four boundaries are adjacent, a configuration whose energy has terms such as $4I_0$, $3I^1(1)$ and $2I^2(2)$ as well as $I^3(3)$, and $|3I^1(1)| + |2I^2(2)|$ is expected to be over thirty times the modulus of the term of interest.

We expect the form of $I(n)$ found to be general, not just because of the extreme regularity of the result n^{1-d} for $d = 1, 2, 3$, but also because of an alternative approach to the deduction of phonon spectra. If the spectrum were to be analysed in terms of lattice waves, only the scattering properties of the boundaries would be important in determining the spectral differences on moving the boundaries. These scattering properties will be qualitatively universal, and we expect our results for the interaction to be so too.

The alternation of sign in the interaction between boundaries, or equivalently the existence of two types of boundary, prevents the system from mapping directly onto the Bak–Bruinsma model. Instead of a devil's staircase, we find a single step—that is, the phase $\langle n\, n+1 \rangle$—to be stable in all cases. Between $\langle 2 \rangle$ and $\langle 3 \rangle$ in 2D and 3D we have found no other stable phase, and one of us (MJR) has checked for the existence of other intermediate phases between $\langle 1 \rangle$ and $\langle 2 \rangle$, and $\langle 3 \rangle$ and $\langle 4 \rangle$, in 2D, and found none. Phases with an odd number of symbols in their Zhdanov notation are also found to be less favoured than those with the same density and an even number of symbols, a result which confirms the prediction of Cheng *et al* [8].

Although we have often referred to SiC in this paper, it must be mentioned that this model is not perfect for SiC. In particular in SiC the stacked layers are displaced by one third of their repeat distance to one side, causing, perhaps, the four-layer term of equation (1) to become more important [14]. Other systems, such as PbI_2, have other complications— in this case the iodide and lead ions form stacking structures in a manner which is almost independent, leading to more freedom than a simple rotation for each layer stacked. A fuller discussion of these results with respect to silicon carbide will be published shortly [19].

Appendix A. 1D chains

In this appendix an analytic proof is presented showing that there is no interactions between changed masses or spring constants on a one-dimensional chain. Such a chain is shown in figure A1, and its equation of motion is
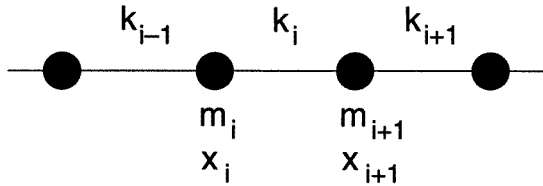
$$\omega^2 u_i = A_{ij} u_j \tag{A1}$$

where

$$u_i = \sqrt{m_i} x_i \tag{A2}$$

and

$$A_{ij} = \begin{cases} (k_{i-1} + k_i)/m_i & j = i \\ -k_i/\sqrt{m_i m_j} & j = i \pm 1. \end{cases} \tag{A3}$$

Figure A1. A chain of balls and springs showing differing masses and spring constants. x_i denotes the displacement from equilibrium.

The important quantity in this analysis is the sum of the logs of the eigenvalues—that is, the Ξ of this paper. This is equivalently the log of the determinant:

$$\Xi = \sum_i \ln(\omega_i^2) = \ln \prod_i (\omega_i^2) = \ln \det \mathbf{A}. \tag{A4}$$

If a matrix $\mathbf{B}$ is defined to be equal to $\mathbf{A}$ but without the factors of m, then as each m_i appears to the power of -0.5 throughout just one row and one column,

$$\det \mathbf{A} = \det \mathbf{B} \prod_i (m_i)^{-1}. \tag{A5}$$

In particular, if $m_i = m_j = M$, and all of the other masses are of value m, then the value of $\det \mathbf{A}$ is independent of $i - j$, the separation of the changed masses. Thus there is no interaction between two changed masses on a 1D chain via the phonon free energy in the high-temperature limit.

In order to consider changes in the ks, it is necessary to transform $\mathbf{B}$ somewhat. $\mathbf{B}$ represents the equations of motion for a system of unit masses, the masses having been factored out of the original matrix $\mathbf{A}$. These equations are as follows:

$$\begin{aligned} -\omega^2 u_i &= k_{i-1} u_{i-1} - (k_{i-1} + k_i) u_i + k_i u_{i+1} \\ -\omega^2 u_{i+1} &= k_i u_i - (k_i + k_{i+1}) u_{i+1} + k_{i+1} u_{i+2}. \end{aligned} \tag{A6}$$

These equations are written twice to ease the transformation from u_i to a coordinate $e_i = u_{i+1} - u_i$, which is achieved by subtracting the first line from the second. Thus:

$$-\omega^2 e_i = k_{i-1} e_{i-1} - 2k_i e_i + k_{i+1} e_{i+1} \tag{A7}$$

or, in matrix form,

$$\omega^2 e_i = C_{ij} e_j \tag{A8}$$

with

$$C_{ij} = \begin{cases} -k_{i-1} & j = i - 1 \\ 2k_i & j = i \\ -k_{i+1} & j = i + 1. \end{cases} \tag{A9}$$

And finally,

$$\det \mathbf{C} = \det \mathbf{D} \prod_i (k_i) \tag{A10}$$

where $\mathbf{D}$ is the matrix with 2 on the leading diagonal, and -1 on the first off-diagonal. So once more $\sum \ln \omega^2$ is independent of the position or relative position of any changed ks.

References

[1] Verma A R and Krishna P 1966 *Polytypism and Polymorphism in Crystals* (New York: Wiley)
[2] Krishna P (ed) 1983 *Progress in Crystal Growth and Characterization* vol 7 (Oxford: Pergamon)
[3] Steinberger I T 1983 *Progress in Crystal Growth and Characterization* vol 7, ed P Krishna (Oxford: Pergamon) p 7
[4] Engel G E 1990 *J. Phys.: Condens. Matter* **2** 6905
[5] Pandey D and Krishna P 1975 *J. Cryst. Growth* **31** 66
[6] Pirouz P, Young J W, Powell J A and Ernst F 1991 *Microscopy of Semiconducting Materials (Inst. Phys. Conf. Ser. 117)* (Bristol: Institute of Physics Publishing) p 149
[7] Jagodzinski H 1954 *Neues Jahrb. Mineral Monatsh.* **3** 49
[8] Cheng C, Heine V and Jones I L 1990 *J. Phys.: Condens. Matter* **2** 5097
[9] Hofmann M, Zywietz A, Karch K and Bechstedt F 1994 *Phys. Rev.* B **50** 13 401
[10] Winkler B, Dove M T, Salje E K H, Leslie M and Palosz B 1991 *J. Phys.: Condens. Matter* **3** 539
[11] Bak P and Bruinsma R 1982 *Phys. Rev. Lett.* **49** 249
[12] Zhdanov G S 1945 *C. R. Acad. Sci., URSS* **48** 43
[13] Cheng C, Needs R J and Heine V 1988 *J. Phys. C: Solid State Phys.* **21** 1049
[14] Shaw J J A and Heine V 1990 *J. Phys.: Condens. Matter* **2** 4351
[15] Yeomans J 1988 *Solid State Physics* vol 41 (New York: Academic) p 151
[16] Aubry S 1983 *J. Phys. C: Solid State Phys.* **16** 2497
[17] Cheng C, Heine V and Needs R J 1990 *J. Phys.: Condens. Matter* **2** 5115
[18] Käckell P, Wenzien B and Bechstedt F 1994 *Phys. Rev.* B **50** 17 037
[19] Rutter M J and Heine V 1997 *J. Am. Ceram. Soc.* to be submitted